Certification of photon Fock states using second-order nonlinearity

Dat Thanh Le [1,2,*] Marcelo P. Almeida [1] and Nguyen Ba An [2,3]

[1]*Australian Research Council Centre of Excellence for Engineered Quantum Systems, School of Mathematics and Physics, University of Queensland, Brisbane QLD 4072, Australia*

[2]*Thang Long Institute of Mathematics and Applied Sciences, Thang Long University, Nghiem Xuan Yem, Hoang Mai, Hanoi 10000, Vietnam*

[3]*Institute of Physics, Vietnam Academy of Science and Technology, 18 Hoang Quoc Viet, Cau Giay, Hanoi 10000, Vietnam*

(Received 11 October 2022; accepted 21 November 2022; published 8 December 2022)

Certifying whether a photon Fock state is present or not while preserving its quantum state is an important task that proves useful in quantum technologies. The existing methods to perform such task apply to single photons only and consume costly quantum resources. In this paper, we propose a resource-efficient scheme for certification of an arbitrary (nonvacuum) photon Fock state by using second-order nonlinearity. In particular, we utilize the correlations in both photon number and polarization of a stimulated parametric downconversion process to herald the presence and the quantum state of an incoming Fock state. The proposed scheme works excellently with a near perfect certification fidelity even when using nonideal photodetectors. We then compare our scheme with the existing ones taking into account relevant figures of merit for each method. We also present applications of our scheme in overcoming transmission loss of photons in quantum channels as well as in preparation of NOON states, $(|N\rangle|0\rangle + |0\rangle|N\rangle)/\sqrt{2}$. Our paper introduces to the optical toolbox a practical technique that is beneficial for quantum communication and quantum metrology.

DOI: 10.1103/PhysRevA.106.062608

I. INTRODUCTION

Quantum nondemolition (QND) measurement of a single photon plays an essential role in overcoming transmission loss in various quantum protocols such as device-independent quantum key distribution [1,2], random number generation [3,4], and tests of Bell inequalities [5,6]. Implementing this kind of measurement often involves an auxiliary probe system coupled to the photon in such a way that the probe's quantum state is dependent on whether or not the photon is present [7]. In that way, measurement on the probe confirms the photon's existence without destroying it and such measurement can be repeated, yielding the same outcome [8]. A well-known proposal following this principle is the use of cross-Kerr effect [9] that induces change in the phase of a probe field with respect to the photon number of a target field. However, this method is inefficient due to the inherently weak third-order nonlinearity and the multimode nature of photons [10,11]. Recently, deterministic QND measurement of a photon has been realized in an advanced cavity-QED system [12–14], where reflection of a photon from a cavity imparts a π shift on the relative phase of an atomic superposition state.

A close variant of the above QND measurement is the so-called certification of a single photon [15], by which the input field is annihilated after measurement but its quantum state is transferred to an auxiliary mode. This task is suitable for quantum protocols, e.g., tests of Bell inequalities, where the input photon waveform is not of interest [13]. To our knowledge, there exist three approaches that have experimentally realized certification of a single photon. The first one exploits spontaneous parametric downconversion (PDC) of the input photon [15,16]. The other two rely on quantum teleportations of single-rail [17,18] and dual-rail [19,20] qubits, respectively. These methods however suffer from several limitations, either yielding a very low certification rate due to the weakness of third-order nonlinearity [16] or consuming costly quantum overheads such as single photons [18] and polarization Bell pairs [20]. Furthermore, the latter two methods necessitate attentive synchronization between distant and indistinguishable photons, thus posing a practical difficulty when implemented with distinct source and receiver.

In this paper, we propose a different scheme based on second-order nonlinearity for certification of photons. We show that stimulated type-II PDC in a nonlinear crystal [21,22] can be employed to certify the presence of an arbitrary (nonvacuum) photon Fock state, i.e., a state containing an arbitrary number of photons. This is possible owing to the intriguing correlations in both photon number and polarization of the downconverted photons that allow one of these modes to resemble the quantum state of the input Fock state. Our scheme offers advantages compared with the existing ones. First, similar to the spontaneous-PDC scheme ours does not involve synchronization or indistinguishability but has a much higher success rate by means of strong second-order nonlinearity. Second, it is resource efficient, requiring neither additional quantum states nor feedforward corrections that are requisite in the existing schemes. Third, keeping the same setup it is applicable not only to single photons but also to arbitrary multiphoton Fock states, $|n_H, (N-n)_V\rangle$, and

*thanhdat.le@uq.net.au

their symmetric superpositions, $\alpha|n_H,(N-n)_V\rangle+\beta|(N-n)_H,n_V\rangle$, where $|m_H,n_V\rangle$ represents a single-mode state that has m horizontal photons and n vertical ones. In addition, our scheme is readily realizable, as experimental demonstrations of stimulated PDC have been shown in numerous works, including quantum cloning of a single photon [23], state preparation of a single-rail qubit [24], and implementation of single-photon addition [25,26].

The outline of this paper is as follows. In Sec. II we reintroduce the three existing methods for certification of a photon and then propose our scheme for an arbitrary Fock state. We also provide detailed comparisons between our scheme and the others. In Sec. III we present two applications of our certification scheme: (i) in overcoming transmission loss of photons in quantum communication and (ii) in generation of NOON states. We conclude our paper in Sec. IV. Three appendices are added to complement the results in the main text.

II. CERTIFICATION OF A PHOTON FOCK STATE

A. Overview of the existing schemes

1. Using spontaneous PDC

The scheme proposed by Cabello and Sciarrino [15] and implemented by Meyer-Scott *et al.* [16] certifies a single photon by splitting it into two via spontaneous PDC (see Appendix A1 for more details of the scheme). One of the downconverted photons is measured in a particular basis, which projects the other one onto a quantum state that is unitarily identical to that of the input photon. Concretely, the input photon is assumed to be in the state

$$|\psi\rangle_{\rm in}=\alpha|H\rangle_{\rm in}+\beta|V\rangle_{\rm in}, \tag{1}$$

where $|\alpha|^2+|\beta|^2=1$ and $|H\rangle\equiv|1_H\rangle$ ($|V\rangle\equiv|1_V\rangle$) is a Fock state containing one photon of horizontal (vertical) polarization. The photon is sent to a waveguide nonlinear crystal with high nonlinearity; with some probability it is downconverted into $|0\rangle_{\rm in}(\alpha|H\rangle_1|H\rangle_2+\beta|V\rangle_1|V\rangle_2)$, where the subscripts 1 and 2 denote the two downconverted modes. Mode 1 is then measured in the diagonal basis, $(|H\rangle_1\pm|V\rangle_1)/\sqrt{2}$. Depending on the outcome of this measurement, mode 2 will be collapsed into $\alpha|H\rangle_2\pm\beta|V\rangle_2$, which is identical to the initial state $|\psi\rangle_{\rm in}$ up to a feedforward Pauli correction. Therefore, the measurement "click" in mode 1 has heralded the presence of $|\psi\rangle_{\rm in}$, while also transferring entirely its qubit state onto the photon in mode 2.

2. Using single-rail quantum teleportation

The second scheme for certification of a single photon is based on quantum teleportation of a single-rail qubit [17,18] (see Appendix A2 for more details of the scheme). To understand this scheme, we first rewrite the input state as $|\psi\rangle_{\rm in}=\alpha|1_H\rangle_{\rm in}|0_V\rangle_{\rm in}+\beta|0_H\rangle_{\rm in}|1_V\rangle_{\rm in}$, which explicitly separates its horizontal and vertical parts. We also prepare auxiliary single-rail entanglements in the form $(\sqrt{1-t}|1_H\rangle_1|0\rangle_2+\sqrt{t}|0\rangle_1|1_H\rangle_2)\otimes(\sqrt{1-t}|1_V\rangle_1|0\rangle_2+\sqrt{t}|0\rangle_1|1_V\rangle_2)$, which are created by sending two photons $|1_H\rangle|1_V\rangle$ to a beam splitter (BS) with transmittance t. This transmittance plays an important role when performing amplification of a lossy single photon using the scheme of interest. The horizontal and vertical parts of $|\psi\rangle_{\rm in}$ are then respectively teleported to mode 2 using the corresponding horizontal and vertical single-rail entanglements as quantum channels. Depending on different outcomes of the Bell-like measurement on mode in and mode 1, an (un-normalized) final state $\pm\alpha\sqrt{t(t-1)}|1_H\rangle_2|0_V\rangle_2\pm\beta\sqrt{t(1-t)}|0_H\rangle_2|1_V\rangle_2$ is obtained, to which application of a feedforward Pauli correction yields the input state $|\psi\rangle_{\rm in}$. Recently, Guanzon *et al.* [27] have proposed a linear-optics scheme to implement ideal quantum teleamplification up to an N-photon Fock state, assisted by N auxiliary single photons and quantum Fourier transform. This scheme can be adapted to certification of an arbitrary Fock state.

3. Using dual-rail quantum teleportation

The third scheme is conceptually simple, certifying the input state $|\psi\rangle_{\rm in}$ by teleporting it to mode 2 of an auxiliary dual-rail Bell pair [19,20], say, $|\Psi^+\rangle_{12}=(|H\rangle_1|V\rangle_2+|V\rangle_1|H\rangle_2)/\sqrt{2}$ (see Appendix A3 for more details of the scheme). The scheme thus requires a Bell measurement on modes in and 1 as well as a Pauli correction conditioned on the measurement outcome.

B. Our scheme using stimulated type-II PDC

Different from the above schemes, in what follows we propose exploiting type-II PDC for certification of an arbitrary photon Fock state. To this end, we examine spontaneous and stimulated PDC processes in a type-II nonlinear crystal in the presence of a strong classical pump field. We analyze the correlations in photon number and polarization of the downconverted photons in both cases. Based on these, we describe our certification scheme and explain its working mechanism.

Type-II second-order interaction in a nonlinear crystal gives rise to spontaneous PDC of a pumping photon into two lower-frequency ones that are called the signal (s) and idler (i) modes. The downconverted photons are orthogonal in polarization and emitted into directions symmetrically oriented relative to that of the pumping beam [28] [see Fig. 1(a)]. This interaction is described by the Hamiltonian [21,29]

$$\hat{H}_{si}=\gamma(\hat{a}^\dagger_{s,H}\hat{a}^\dagger_{i,V}+\hat{a}^\dagger_{s,V}\hat{a}^\dagger_{i,H})+\text{H.c.}, \tag{2}$$

where γ is the coupling strength proportional to second-order nonlinearity as well as the intensity of the classical pump and $\hat{a}^\dagger_{m,p}$ is the creation operator of the photon in mode $m\in\{s,i\}$ with polarization $p\in\{H,V\}$. $\hat{H}_{si}$ is an effective squeezing interaction between the signal and idler modes, resulted from a three-wave mixing process when the pump is treated classically. These modes are required to fulfill the phase-matching conditions, including conservations of momentum and energy [30]. The time evolution of $\hat{H}_{si}$ is

$$\hat{S}_{si}=\exp(\xi\hat{K}^\dagger_{si}-\xi^*\hat{K}_{si}), \tag{3}$$

where $\hat{K}^\dagger_{si}=\hat{a}^\dagger_{s,H}\hat{a}^\dagger_{i,V}+\hat{a}^\dagger_{s,V}\hat{a}^\dagger_{i,H}$ and $\xi=-i\gamma\tau/\hbar$ with τ the interacting time. $\hat{S}_{si}$ is sometimes referred to as a type-II two-mode squeezer [31]. We introduce an input-output relation via

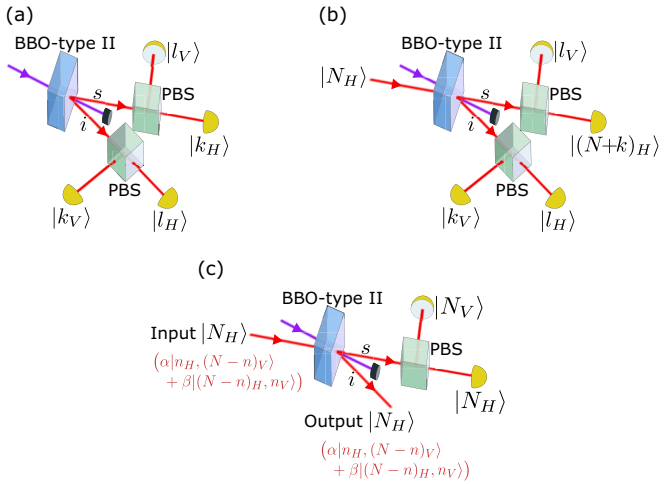

FIG. 1. (a) Schematic of spontaneous type-II PDC, where a photon from the pumping beam is split into two daughter photons in the signal (s) and idler (i) modes. Photon detections in these two modes show the nonclassical correlations in their photon number and polarization: If mode s is found in $|k_H, l_V\rangle_s$, then mode i will be $|l_H, k_V\rangle_i$, and vice versa. (b) Schematic of stimulated type-II PDC, where a seed Fock state $|N_H\rangle$ is injected to mode s. The correlations of photons in modes s and i remain the same as in (a) except now mode s after the stimulated process has N horizontal photons more. (c) Our scheme for certification of an arbitrary photon Fock state. From the correlations shown in (b), one sees that photon detection of mode s in the state $|N_H, N_V\rangle_s$, which corresponds to $k = 0$ and $l = N$, will project mode i exactly onto the state $|N_H\rangle_i$. This effectively certifies the seed Fock state in mode s without annihilating it. The setup also works for a symmetric Fock-state superposition $\alpha|n_H, (N-n)_V\rangle + \beta|(N-n)_H, n_V\rangle$.

application of $\hat{S}_{si}$ [32]:

$$\hat{S}_{si}|m_H, n_V\rangle_s|0\rangle_i = \sum_{k,l=0}^{\infty} c_{m,n}^{k,l}|(m+k)_H,(n+l)_V\rangle_s|l_H,k_V\rangle_i, \tag{4}$$

where

$$c_{m,n}^{k,l} = (-i\Gamma)^{k+l} K_{m+n}\left(C_{m+k}^{m} C_{n+l}^{n}\right)^{1/2}, \tag{5}$$

with $\Gamma = \tanh(i\xi)$ the squeezing parameter, $K_n = (1-|\Gamma|^2)^{(n+2)/2}$ a function of $|\Gamma|$, and $C_n^k = n!/[(n-k)!k!]$.

Following Eq. (4), the output state in modes s and i resulted from spontaneous PDC is given by

$$\hat{S}_{si}|0\rangle_s|0\rangle_i = \sum_{k,l=0}^{\infty} c_{0,0}^{k,l}|k_H, l_V\rangle_s|l_H, k_V\rangle_i, \tag{6}$$

which shows clearly the correlations in number and polarization of photons in modes s and i. Particularly, mode s has k horizontal photons and l vertical ones, while it is vice versa for mode i that has l horizontal photons and k vertical ones. Therefore, photon detection on one mode will disclose the quantum state of the other mode. We demonstrate these correlations in Fig. 1(a). Of particular interest is the case when $k + l = 1$, i.e., the system emits pairs of single photons. Detection of a single photon in one mode then guarantees the existence of a single photon in the other mode. This constitutes the most widely used single-photon sources [33,34].

Instead of spontaneous PDC, stimulated PDC occurs in a type-II second-order nonlinear crystal when injecting a seed light field to mode s or/and mode i [25,26]. As shown in Fig. 1(b), we consider sending a horizontal N-photon input state, $|N_H\rangle_{\text{in}}$, to mode s. The corresponding stimulated-PDC output following Eq. (4) reads

$$\hat{S}_{si}|N_H\rangle_s|0\rangle_i = \sum_{k,l=0}^{\infty} c_{N,0}^{k,l}|(N+k)_H, l_V\rangle_s|l_H, k_V\rangle_i. \tag{7}$$

In Eq. (7) photons in mode s and i remain correlated in the same fashion as in Eq. (6), except that now mode s has N more horizontal photons that originate from the seed Fock state. Intriguingly, one observes from Eq. (7) that if mode s is detected in the state $|N_H, N_V\rangle_s$, which imposes $k = 0$ and $l = N$, mode i will be collapsed into $|N_H\rangle_i$, which is identical to the initial input Fock state. Therefore, the measurement on mode s has confirmed the presence of such input Fock state. Its original physical state is destroyed but its quantum state is sent perfectly to mode i. This presents the underlying mechanism in our Fock-state certification scheme as depicted in Fig. 1(c). Markedly, our scheme can also certify a vacuum input state. In this case, our proposed setup is identified with the conventional spontaneous PDC with a strong coherent pump, in which no photons detected in mode s or i imply a vacuum state in the other mode. Recently, it has been shown that detection of zero photons might benefit some quantum information applications [35].

In a similar manner, one can check that the above certification holds when the initial input state seeded to mode s contains also vertical photons, for example, in the form $|n_H, (N-n)_V\rangle_{\text{in}}$ or $|(N-n)_H, n_V\rangle_{\text{in}}$ with $n \leqslant N$. Remarkably, the symmetry between horizontal and vertical modes in stimulated type-II PDC [see the interaction in Eq. (2)] allows our certification scheme to work even for an arbitrary superposition of these Fock states:

$$|\psi_{N,n}\rangle_{\text{in}} = \alpha|n_H, (N-n)_V\rangle_{\text{in}} + \beta|(N-n)_H, n_V\rangle_{\text{in}}. \tag{8}$$

Indeed, taking $|\psi_{N,n}\rangle_{\text{in}}$ as the seed state in mode s and using Eq. (4) we find the corresponding stimulated-PDC output:

$$\alpha \sum_{k,l=0}^{\infty} c_{n,N-n}^{k,l}|(n+k)_H, (N-n+l)_V\rangle_s|l_H, k_V\rangle_i$$
$$+\beta \sum_{k',l'=0}^{\infty} c_{N-n,n}^{k',l'}|(N-n+k')_H, (n+l')_V\rangle_s|l'_H, k'_V\rangle_i. \tag{9}$$

Within this state, detection of mode s in $|N_H, N_V\rangle_s$ implies $k = N-n$, $l = n$, $k' = n$, and $l' = N-n$ and hence projects mode i exactly into the state $|\psi_{N,n}\rangle$ in Eq. (8). The success probability of our certification scheme for this general input state is

$$P_{N,n} = \left|c_{n,N-n}^{N-n,n}\right|^2 = |\Gamma|^{2N}(K_N)^2\left(C_N^n\right)^2. \tag{10}$$

For $N = n = 1$ this amounts to certification of a single photon with the success probability $P_{N=1,n=1}$, which is of order 10^{-4}–10^{-2} for a typical value of the squeezing parameter $|\Gamma| \approx 10^{-2}$–10^{-1} [29].

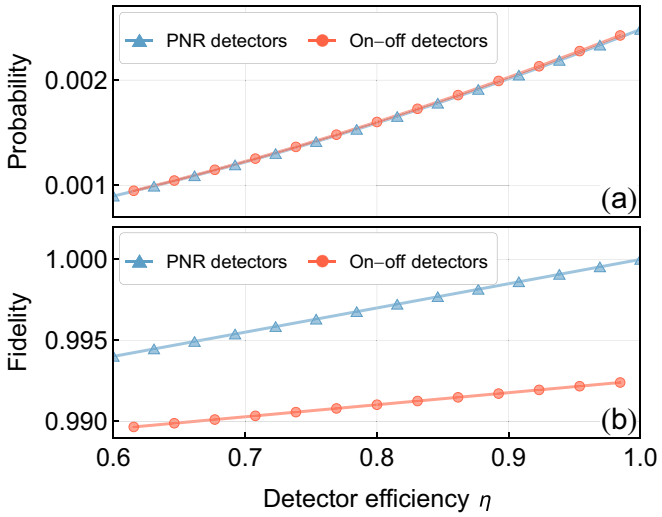

FIG. 2. (a) Success probability and (b) fidelity between the certified output state and the input state of our scheme when certifying a single photon as functions of the detector efficiency η. We consider using both PNR (marked by filled triangles) and on-off (marked by filled circles) detectors. Here the squeezing parameter $|\Gamma|$ is chosen to be 0.05.

It deserves noting that our scheme can certify the presence of an arbitrary symmetric two-mode N-photon state of the form $\alpha|n_{P_1}\rangle_1|(N-n)_{P_2}\rangle_2 + \beta|(N-n)_{P_1}\rangle_1|n_{P_2}\rangle_2$, where mode 1 has polarization P_1 which can be horizontal or vertical and similarly for mode 2 with polarization P_2. This is because of the equivalence between path and polarization degrees of freedom (DOFs), by which a linear-optics transformation can recast such two-mode state into a one-mode N-photon Fock state, i.e., the state in Eq. (8). For example, when $P_1 = H$ and $P_2 = V$, a polarizing beam splitter transforms the state $\alpha|n_H\rangle_1|(N-n)_V\rangle_2 + \beta|(N-n)_H\rangle_1|n_V\rangle_2$ into $\alpha|n_H, (N-v)_V\rangle_2 + \beta|(N-n)_H, n_V\rangle_1$. The symmetric two-mode N-photon state has proven useful in achieving the quantum Cramér-Rao bound of phase estimation in conventional two-path interferometers [36].

Our certification scheme in general demands photon-number-resolving (PNR) detectors to perform precisely the detection $|N_H, N_V\rangle_s$ in mode s. However, for the case of certification of a single photon, on-off detectors that only distinguish between vacuum and nonvacuum states suffice for our scheme. This is because the squeezing parameter $|\Gamma|$ is typically small, making higher-order terms in the stimulated-PDC output in Eq. (7) or Eq. (9) with mode s having more than two photons in horizontal and/or vertical polarizations insignificant compared with lower-order terms. Namely, for $|\Gamma| \ll 1$ it can be verified that the output state in Eq. (9) is very well approximated to

$$c_{1,0}^{0,0}|\psi_{N=1,n=1}\rangle_s|0\rangle_i + c_{1,0}^{0,1}|1_H, 1_V\rangle_s|\psi_{N=1,n=1}\rangle_i + \alpha c_{1,0}^{1,0}|2_H, 0_V\rangle_s|0_H, 1_V\rangle_i + \beta c_{0,1}^{0,1}|0_H, 2_V\rangle_s|1_H, 0_V\rangle_i,$$

in which higher-order terms with mode s being in $|k_H, l_V\rangle$ $(k + l > 2)$ are absent.

In Fig. 2 we examine the performance of our certification scheme for a single photon using both PNR and on-off detectors. Mathematical models for these detectors are presented in Appendix B. We assume the squeezing parameter to be $|\Gamma| = 0.05$ and plot our scheme's success probability and the fidelity between the output certified state and the input single photon versus the detector efficiency η. One observes from Fig. 2(a) that the success probability is virtually the same for both types of photodetectors, varying from near 0.001 to above 0.002. Meanwhile, Fig. 2(b) shows that the fidelity in both cases is excellently high, larger than 0.99 for $\eta \gtrsim 0.6$. These justify the use of just on-off detectors in our certification scheme for a single photon.

In Appendix B we reiterate the above analysis for certification of an N-photon Fock state with $N \in \{2, 3\}$. We find that in this multiphoton scenario PNR detectors are utterly needed to realize a high-fidelity certification, which is in contrast to the single-photon scenario. We also compute the probability and the certification fidelity of our scheme for different values of the squeezing parameter $|\Gamma|$ in Appendix B. We observe that for $|\Gamma| \ll 1$, the probability is substantially reduced when decreasing the PNR detection efficiency; however, the certification fidelity remains close to 1. This is understandable, since in such limit high-photon-number terms in mode s of the stimulated-PDC output are negligible compared to the target detection term $|N_H, N_V\rangle_s$, which results in a very small false-detection probability and thus a very high certification fidelity. Realistically nonideal PNR detectors are thus sufficient for a high-quality multiphoton certification using our scheme.

C. Comparisons with the existing schemes

Table I shows the comparisons between our certification scheme and the existing ones in terms of various characteristics for each method. To facilitate our discussion, from now on we refer to the spontaneous-PDC scheme as $\mathcal{C}_1$, the single-rail teleportation based scheme as $\mathcal{C}_2$, and the dual-rail teleportation based scheme as $\mathcal{C}_3$.

Regarding the working mechanism, our scheme puts forward a totally different approach to certifying photon Fock states, that is, we utilize stimulated type-II PDC. This gives us two immediate advantages compared with the schemes $\mathcal{C}_j$ $(j = 1, 2, 3)$. First, making use of second-order nonlinearity, which is much stronger than third-order nonlinearity as in $\mathcal{C}_1$, will substantially improve the certification rate. Second, in contrast to $\mathcal{C}_2$ and $\mathcal{C}_3$ our scheme does not rely on interference, so synchronization of indistinguishable, distant photons that requires fine temporal, spatial, and spectral overlaps is irrelevant. This is highly desirable when the incoming photon source is far away from the detection location. Despite sharing a similar PDC characteristic, our scheme is very different from $\mathcal{C}_1$. In particular, $\mathcal{C}_1$ is based on a three-wave mixing process, which probabilistically down-converts the input single photon into two lower-frequency photons. Meanwhile, ours relies on a squeezing interaction between the signal and idler modes that gives rise to their nontrivial correlations in photon number and polarization.

As for the resources needed, our scheme involves a type-II second-order nonlinear crystal and photodetectors. While the latter are indispensable in all implementations, the former is more readily available and economical than third-order

TABLE I. Comparisons between our photon certification scheme and the existing ones, namely, the spontaneous-PDC scheme and the two schemes using quantum teleportations of single-rail and dual-rail qubits, in terms of synchronization, resource requirement, photodetector type, feedforward correction, order of success probability, and applicability. Our scheme features a simplicity in experimental hardware, acceptable success probability, and applicability to arbitrary Fock states. Here the success probabilities of the two teleportation based schemes are respectively estimated for on-demand (i.e., deterministic) and probabilistic resources of auxiliary quantum states. Our scheme's success probability and that of the single-rail teleportation scheme are estimated only for single-photon certification.

	Synchronization	Resource requirement	Photodetector type	Feedforward correction	Order of success probability	Applicability
Using spontaneous PDC [15,16]	Not required	Third-order nonlinearity	On-off	Required	$\approx 10^{-8}$	Single photons
Using single-rail teleportation [17,18,27]	Required	N auxiliary single photons	PNR	Required	$\approx 10^{-1}$ or $\approx 10^{-4}$	Arbitrary Fock states
Using dual-rail teleportation [19,20]	Required	An auxiliary Bell pair	On-off	Required	$\approx 10^{-1}$ or $\approx 10^{-4}$	Single photons
Our scheme using stimulated PDC	Not required	Second-order nonlinearity	On-off ($N=1$) or PNR ($N>1$)	Not required	$\approx 10^{-4} - 10^{-2}$	Arbitrary Fock states

nonlinearity as in $\mathcal{C}_1$, auxiliary single photons as in $\mathcal{C}_2$, or an auxiliary polarization Bell pair as in $\mathcal{C}_3$, which are expensive quantum resources. For certifying a single photon, our scheme requires only on-off detectors for a reliable operation. For that of a multiphoton Fock state PNR detectors are requisite in our scheme. PNR detectors are currently available, which can be realized via superconducting transition edge sensors [37–39], multiplexing of single-photon detectors [40–43], or analyses of output signal waveforms [44]. Moreover, our scheme works without feedforward corrections that are vital in the existing schemes, which will reduce the hardware complexity of a realistic implementation of our scheme. In fact, highly similar setups to our proposed scheme that use stimulated PDC have been realized in various experiments, for example, in implementing single-photon addition [25,26].

Based on our estimates, our scheme's success probability (and therefore the certification rate) is several orders of magnitude higher than that of $\mathcal{C}_1$. It is much lower than those of $\mathcal{C}_2$ and $\mathcal{C}_3$ in an idealized situation where the auxiliary quantum states (i.e., N single photons in $\mathcal{C}_2$ and a polarization Bell pair in $\mathcal{C}_3$) are on demand, but is comparable in a more typical situation where they are probabilistically supplied. One way to further boost the success probability of our scheme is to increase the coherent pump amplitude [45,46]. This however could amplify the undesired effect from higher-order multiphoton terms (see Appendix B for an analysis of such effect).

Another salient feature of our scheme is its applicability to arbitrary Fock states and their symmetric superpositions while keeping the same experimental setup. These nonclassical states are a key resource in many quantum metrology protocols [47–51]. As will be shown later, using our certification method we derive a scheme for preparation of NOON states for arbitrary N.

III. APPLICATIONS

A. Overcoming transmission loss in quantum channels

We consider a realistic scenario when the pure single photon $|\psi\rangle_{\text{in}}$ in Eq. (1) is sent through a lossy quantum channel. Experiencing photon loss, it becomes a mixed state with a non-negligible vacuum component [18]:

$$\hat{\rho}_{\text{in}} = \delta_0 |0\rangle_{\text{in}}\langle 0| + \delta_1 |\psi\rangle_{\text{in}}\langle\psi|, \tag{11}$$

where δ_0 and δ_1 are real positive satisfying $\delta_0 + \delta_1 = 1$ and $\delta_0 > \delta_1$ for a heavily lossy channel. The scheme of certification of a single photon can mitigate this effect of transmission loss. In fact, it can act as a noiseless single-photon amplifier [27,52,53] that amplifies the single-photon component in Eq. (11) compared to the vacuum one, i.e., increasing the weight ratio δ_1/δ_0, thus making the mixed state $\hat{\rho}_{\text{in}}$ close enough to the initial pure single photon $|\psi\rangle_{\text{in}}$.

Our certification scheme is also suitable for this purpose. Specifically, we consider the mixed state $\hat{\rho}_{\text{in}}$ in Eq. (11) as the seed state in mode s of the setup in Fig. 1(c). We find the stimulated-PDC output in this case as

$$\hat{S}_{si}(\delta_0 |0\rangle_s\langle 0| + \delta_1 |\psi\rangle_s\langle\psi|)|0\rangle_i\langle 0|\hat{S}_{si}^{\dagger}, \tag{12}$$

where $\hat{S}_{si}$ is given in Eq. (3). Upon detecting mode s in the state $|1_H, 1_V\rangle_s$, mode i will be projected onto an (unnormalized) mixed state:

$$\delta_0 |\Gamma|^4 (K_0)^2 |1_H, 1_V\rangle_i\langle 1_H, 1_V| + \delta_1 |\Gamma|^2 (K_1)^2 |\psi\rangle_i\langle\psi|. \tag{13}$$

Comparing Eq. (13) to Eq. (11),[1] one sees that the vacuum component has been replaced by a two-photon term and the two initial weights, δ_0 and δ_1, have been modified. The weight ratio between the single-photon component and the two-photon one in Eq. (13) is given by $|\Gamma|^{-2}(K_1/K_0)^2 \times (\delta_1/\delta_0) \approx 10^4 \times (\delta_1/\delta_0)$ for $|\Gamma| \approx 10^{-2}$ (note here that $K_1 \approx K_0$ for $|\Gamma| \ll 1$). This shows amplification of the single-photon component in the output mixed state with a gain factor of $\approx\sqrt{10^4} = 10^2$.

[1]Note the change in the subscript notation from in to i, which follows our notation use in Fig. 1, i.e., the input state (mode in) is seeded to mode s and the output certified state is in mode i.

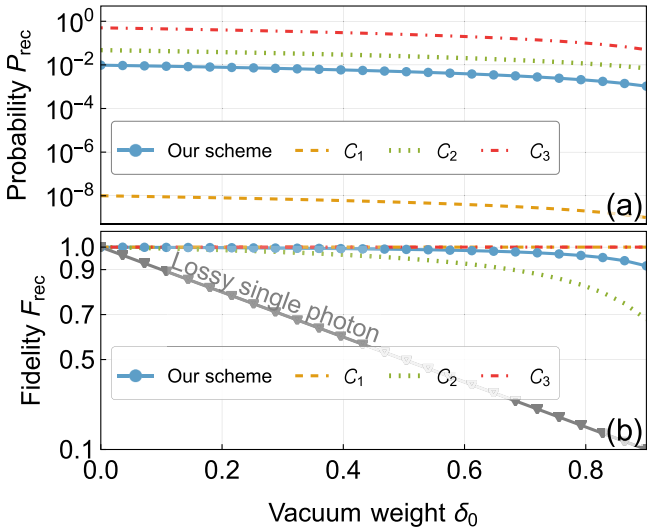

FIG. 3. (a) Success probability $P_{\rm rec}$ given in Eq. (14), and (b) fidelity $F_{\rm rec}$ given in Eq. (15) (both marked by filled circles) as functions of the vacuum weight δ_0 for recovery of a lossy single photon given in Eq. (11), using our certification scheme. We also plot the probabilities and the fidelities when using the three existing certification schemes $\mathcal{C}_j$ $(j = 1, 2, 3)$. In (b) the fidelities of the schemes $\mathcal{C}_1$ and $\mathcal{C}_3$ are exactly 1. We also plot the fidelity of the lossy single photon in Eq. (11), which decreases linearly with δ_0. Here the squeezing parameter $|\Gamma|$ is chosen to be 0.1.

The success probability and the fidelity for recovery of this lossy single-photon input are respectively

$$P_{\rm rec} = \delta_0|\Gamma|^4(K_0)^2 + \delta_1|\Gamma|^2(K_1)^2, \tag{14}$$

$$F_{\rm rec} = \frac{1}{(\delta_0/\delta_1)|\Gamma|^2(K_0/K_1)^2 + 1}. \tag{15}$$

The fidelity $F_{\rm rec}$ does not depend on the coefficients of the input single photon $|\psi\rangle_{\rm in}$, α and β. This agrees with the fact that our certification scheme works in the same manner for a single photon of arbitrary polarization, due to the symmetry between the horizontal and vertical modes in the type-II squeezing interaction in Eq. (2). For $|\Gamma| \ll 1$ and $\delta_1/\delta_0 \gg \mathcal{O}(|\Gamma|^2)$, one finds $F_{\rm rec}$ is very close to 1, indicating that our certification scheme is capable of recovering almost perfectly a single photon that was affected by transmission loss. In Fig. 3 we plot $P_{\rm rec}$ and $F_{\rm rec}$ as functions of the vacuum weight δ_0, which is commensurate with how lossy a quantum channel is. We also plot the probabilities and the fidelities when using the other certification schemes $\mathcal{C}_j$ $(j = 1, 2, 3)$ to recover a lossy single photon (we compute and estimate these in Appendix A).

From Fig. 3(a), it is seen that the probability $P_{\rm rec}$ reduces from 10^{-2} to near 10^{-4} when increasing δ_0, which is five to six orders of magnitude higher than that of the scheme $\mathcal{C}_1$ and one to two orders of magnitude lower than those of the schemes $\mathcal{C}_2$ and $\mathcal{C}_3$ (here we assume that the required auxiliary quantum states in $\mathcal{C}_2$ and $\mathcal{C}_3$ are supplied on demand). This is consistent with the estimates shown in Table I. In Fig. 3(b), the fidelity $F_{\rm rec}$ remains above 0.9 for the whole range of δ_0, while that of the scheme $\mathcal{C}_2$ decreases relatively quickly to below 0.7. We note that the schemes $\mathcal{C}_1$ and $\mathcal{C}_3$ under ideal conditions restore a lossy single photon perfectly, so the fidelities of these schemes are exactly 1. In Fig. 3(b), we also plot the fidelity of the lossy single photon in Fig. (11), which without resorting to any certification schemes quickly reduces to near zero when increasing the vacuum weight δ_0.

An extended, practical scenario relevant to the above is when the single photon that undergoes loss in a quantum channel is entangled with another mode, say, in the form

$$|\Psi\rangle_{{\rm in},a} = \alpha|1_H\rangle_{\rm in}|\phi\rangle_a + \beta|1_V\rangle_{\rm in}|\theta\rangle_a, \tag{16}$$

where $|\phi\rangle_a$ and $|\theta\rangle_a$ are assumed to be orthogonal to each other. Transmission loss in the single-photon part, i.e., mode in, changes the state $|\Psi\rangle_{{\rm in},a}$ into [54]

$$\begin{aligned}&(\delta_0|0\rangle_{\rm in}\langle 0| + \delta_1|1_H\rangle_{\rm in}\langle 1_H|)|\alpha|^2|\phi\rangle_a\langle\phi| \\ &+ (\delta_0|0\rangle_{\rm in}\langle 0| + \delta_1|1_V\rangle_{\rm in}\langle 1_V|)|\beta|^2|\theta\rangle_a\langle\theta| \\ &+ \delta_1(\alpha\beta^*|1_H\rangle_{\rm in}\langle 1_V||\phi\rangle_a\langle\theta| + \alpha^*\beta|1_V\rangle_{\rm in}\langle 1_H||\theta\rangle_a\langle\phi|).\end{aligned} \tag{17}$$

We apply our certification scheme to the single photon in mode in; repeating the calculations in Eqs. (12) and (13) we find that the mixed state in Eq. (17) is transformed to

$$\begin{aligned}&\delta_0|\Gamma|^4(K_0)^2|1_H, 1_V\rangle_i\langle 1_H, 1_V|(|\alpha|^2|\phi\rangle_a\langle\phi| + |\beta|^2|\theta\rangle_a\langle\theta|) \\ &+ \delta_1|\Gamma|^2(K_1)^2|\Psi\rangle_{i,a}\langle\Psi|.\end{aligned} \tag{18}$$

The fidelity between this mixed state and the initial entangled state in Eq. (16) is given by $F_{\rm rec}$ in Eq. (15), which as shown in Fig. 3(b) can be made close to 1 under suitable conditions. To quantify the degree of quantum entanglement retained by the output state after entanglement purification, we use coherent quantum information $I_e = S(\rho_{Q'}) - S(\rho_{RQ'})$ [55,56], where $S(\rho) = -{\rm Tr}(\rho\log_2\rho)$ denotes the von Neumann entropy of a density matrix ρ and Q' and R denote the purified and reference modes [i.e., mode i and mode a in Eq. (18), respectively]. Considering a maximally entangled input state $|\Psi\rangle_{{\rm in},a}$ with $|\alpha| = |\beta| = 1/\sqrt{2}$, we find that $I_e = 2F_{\rm rec} - 1$. For $F_{\rm rec}$ close to 1, I_c is also close to 1, which therefore shows that our certification scheme can distill entanglement after one of its modes is affected by transmission loss. This will be of importance for approaching the ultimate end-to-end rates of a lossy quantum communication network [57].

B. Preparation of NOON states

NOON states, given in the form of a maximally path-entangled state

$$|N :: 0\rangle = \frac{1}{\sqrt{2}}(|N\rangle|0\rangle + |0\rangle|N\rangle), \tag{19}$$

are particularly useful in quantum metrology. They allow for surpassing the shot-noise limit in estimation of a phase shift [58] and beating the Rayleigh limit in optical lithography [59]. There exist methods to generate such states but they are postselected, destroying the prepared state [60–62] or consuming more quantum resources with increasing N [63–66]. Here harnessing our Fock-state certification scheme we propose to prepare NOON states in a heralded fashion and for arbitrary N using the same resources.

Our preparation scheme starts by considering the following *polarized* Schrödinger cat state:

$$|\mathrm{Cat}_\mu\rangle = \mathcal{N}_\mu(|\mu_H\rangle + e^{i\varphi}|-\mu_V\rangle), \tag{20}$$

where $N_\mu = [2(1+\cos(\varphi)e^{-\mu^2})]^{-1/2}$ is a normalization factor and $|\mu_{H/V}\rangle = \sum_{n=0}^{\infty} d_{n,\mu}|n_{H/V}\rangle$ represents a horizontally or vertically polarized coherent state of real amplitude μ with the coefficient $d_{n,\mu} = e^{-\mu^2/2}\mu^n/\sqrt{n!}$. In our previous works [31,54] we have shown how to generate this cat state via interference of a conventional Schrödinger cat state and a coherent state. We reexpress $|\mathrm{Cat}_\mu\rangle$ explicitly in the Fock-state basis:

$$|\mathrm{Cat}_\mu\rangle = \mathcal{N}_\mu \sum_{n=0}^{\infty} d_{n,\mu}(|n_H\rangle + e^{i\varphi}(-1)^n|n_V\rangle). \tag{21}$$

We see that $|\mathrm{Cat}_\mu\rangle$ is a superposition of the states

$$|n_H\rangle + e^{i\varphi}(-1)^n|n_V\rangle,$$

which under a simple linear-optics transformation can be brought to NOON states of the form $\propto (|n_{H/V}\rangle|0\rangle + e^{i\varphi}(-1)^n|0\rangle|n_{H/V}\rangle)$. The decomposition in Eq. (21) thus suggests that we can prepare a NOON state by filtering out the N-photon component in the state $|\mathrm{Cat}_\mu\rangle$ via our certification scheme.

Particularly, we replace the input state $|N_H\rangle$ in Fig. 1(c) with the $|\mathrm{Cat}_\mu\rangle$ in Eq. (21). Using Eq. (4) we find the corresponding stimulated-PDC output state:

$$\mathcal{N}_\mu \sum_{n,k,l=0}^{\infty} d_{n,\mu}\big(c_{n,0}^{k,l}|(n+k)_H, l_V\rangle_s|l_H, k_V\rangle_i + e^{i\varphi}(-1)^n c_{0,n}^{k,l}|k_H, (n+l)_V\rangle_s|l_H, k_V\rangle_i\big). \tag{22}$$

Within this output, we measure mode s in the state $|N_H, N_V\rangle_s$, which collapses mode i into the following (un-normalized) state:

$$\mathcal{N}_\mu \sum_{n=0}^{N} d_{n,\mu}\big(c_{n,0}^{N-n,N}|N_H, (N-n)_V\rangle_i + e^{i\varphi}(-1)^n c_{0,n}^{N,N-n}|(N-n)_H, N_V\rangle_i\big). \tag{23}$$

This state is expectedly close to the "NOON" state $(|N_H\rangle + e^{i\varphi}(-1)^N|N_V\rangle)/\sqrt{2}$.

The success probability and the fidelity for this NOON-state preparation are respectively

$$P_{\mathrm{NOON}} = 2\mathcal{N}_\mu^2\left(2\left|d_{0,\mu}c_{0,0}^{N,N}\right|^2 + \sum_{n=1}^{N}\left|d_{n,\mu}c_{n,0}^{N-n,N}\right|^2\right), \tag{24}$$

$$F_{\mathrm{NOON}} = \frac{\left|d_{N,\mu}c_{N,0}^{0,N}\right|^2}{2\left|d_{0,\mu}c_{0,0}^{N,N}\right|^2 + \sum_{n=1}^{N}\left|d_{n,\mu}c_{n,0}^{N-n,N}\right|^2}. \tag{25}$$

In Fig. 4, we plot P_{NOON} and F_{NOON} versus the cat-state amplitude μ for $N \in \{2, 3, 4\}$, given the other parameters chosen as $\varphi = 0$ and $|\Gamma| = 0.1$. We observe that P_{NOON} and F_{NOON} behave differently when increasing μ. The former initially tends towards an optimal value and then decreases, while the latter approaches 1. Notably, starting from a moderate amplitude $\mu \approx 1.25$, the fidelity F_{NOON} is greater than 0.9 for all $N \in \{2, 3, 4\}$, thus implying that our preparation scheme is capable of generating high-quality NOON states. However,

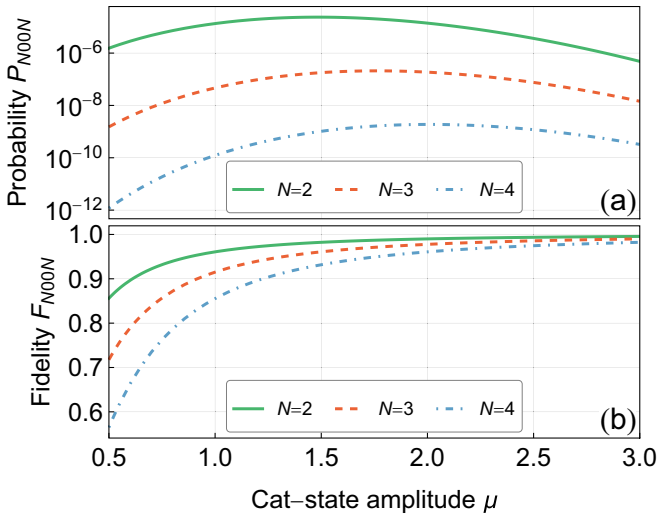

FIG. 4. (a) Success probability P_{NOON} given in Eq. (24) and (b) fidelity F_{NOON} given in Eq. (25), for generation of a NOON state with $N \in \{2, 3, 4\}$ as functions of the cat-state amplitude μ. Here we have chosen $\varphi = 0$ and $|\Gamma| = 0.1$.

the success probability P_{NOON} will likely need to be improved to realize a high-rate NOON-state generation.

It deserves noting that in the presence of loss NOON states decohere rapidly and subsequently lose their ability in achieving super-resolution and supersensitivity [67–69]. To fight against this loss effect, we apply our Fock-state certification scheme to recover lossy NOON states. In Appendix C we show that our scheme restores, with fidelity as high as 0.9 or even higher, NOON states for $N \in \{2, 3, 4\}$ that had undergone loss up to a considerable amount.

IV. CONCLUSIONS

We proposed a scheme to certify arbitrary photon Fock states and their symmetric superposed states without destroying their quantum states. This is achieved via our use of the nontrivial correlations in both photon number and polarization of the downconverted photons in stimulated type-II PDC. We showed that our scheme is superior to the existing ones in terms of resource consumption, hardware complexity, success probability, and applicability. In particular, our scheme can be realized using one type-II second-order nonlinear crystal and efficient photodetectors, which are common devices in quantum-optics experiments. The success probability of our scheme could be much higher or comparable to those of the existing ones. Furthermore, our scheme finds applications not only in fighting against transmission loss of single photons in lossy quantum channels but also in preparation of multiphoton NOON states. A realistic implementation of our scheme is therefore of high interest in quantum communication as well as quantum metrology.

A subsequent study that follows up the present paper will be consideration of applying our certification scheme to specific quantum tasks such as quantum key distribution [17,70] and tests of Bell inequalities [15,16]. Investigation of our NOON-state preparation scheme in a practical situation

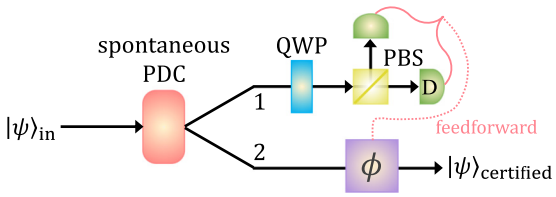

FIG. 5. Certification of a single photon using spontaneous PDC. The input photon $|\psi\rangle_{\text{in}}$ given in Eq. (1) sent to a nonlinear crystal, where polarization-preserving parametric downconversion occurs, is probabilistically downconverted into a pair of photons in modes 1 and 2. The photon in mode 1 is measured in the diagonal basis using a quarter-wave plate (QWP), which certifies the photon in mode 2 that now carries the quantum state of the input photon. The scheme requires a phase feedforward correction (ϕ) on mode 2.

when using an approximate resource as the input polarized Schrödinger cat state [54] is also of interest.

ACKNOWLEDGMENTS

D.T.L. and M.P.A. are supported by the Australian Research Council Centre of Excellence for Engineered Quantum Systems (Grant No. CE170100009), and N.B.A. is supported by the National Foundation for Science and Technology Development under Project No. 103.01-2019.313. We thank Xuemei Gu for discussions at the early-stage development of this manuscript and the referees for useful comments.

APPENDIX A: EXISTING SCHEMES FOR CERTIFICATION OF A SINGLE PHOTON

1. Using spontaneous PDC

The schematic setup of the single-photon certification scheme using spontaneous PDC [15,16] is shown in Fig. 5. The input photon $|\psi\rangle_{\text{in}} = \alpha|H\rangle_{\text{in}} + \beta|V\rangle_{\text{in}}$ is sent to a waveguide nonlinear crystal arranged in such a way that the interaction is of the form

$$\hat{H} = i\hbar\chi(\hat{a}_{\text{in},H}\hat{a}^{\dagger}_{1,H}\hat{a}^{\dagger}_{2,H} + \hat{a}_{\text{in},V}\hat{a}^{\dagger}_{1,V}\hat{a}^{\dagger}_{2,V}) + \text{H.c.}, \tag{A1}$$

where χ determines the nonlinearity strength. This Hamiltonian describes a process that annihilates a single photon in mode in with polarization $p \in \{H, V\}$ while it creates two photons in modes 1 and 2 of the same polarization. We note that when the input field is not a single photon but a strong coherent state and thus can be treated classically, the interaction in Eq. (A1) reduces to $\hat{H} \propto (\hat{a}^{\dagger}_{1,H}\hat{a}^{\dagger}_{2,H} + \hat{a}^{\dagger}_{1,V}\hat{a}^{\dagger}_{2,V}) + \ldots$, which is similar to the Hamiltonian in Eq. (2).

The time evolution of this interaction, $\exp(-i\hat{H}\tau/\hbar)$, applying to the initial total input $(\alpha|1_H, 0_V\rangle_{\text{in}} + \beta|0_H, 1_V\rangle_{\text{in}})|0_H, 0_V\rangle_1|0_H, 0_V\rangle_2$ yields the output

$$\begin{aligned}|\Omega\rangle_{\text{in}12} = {} & \cos(g)(\alpha|H\rangle_{\text{in}} + \beta|V\rangle_{\text{in}})|0\rangle_1|0\rangle_2 \\ & + \sin(g)|0\rangle_{\text{in}}(\alpha|H\rangle_1|H\rangle_2 + \beta|V\rangle_1|V\rangle_2),\end{aligned} \tag{A2}$$

where $g = \chi\tau \ll 1$ is the nonlinear gain. Mode 1 is measured in the diagonal basis, $(|H\rangle_1 \pm |V\rangle_1)/\sqrt{2}$. This projects mode 2 onto the state $\alpha|H\rangle_2 \pm \beta|V\rangle_2$, which is unitarily identical to the initial state $|\psi\rangle_{\text{in}}$. The total success probability of this scheme is

$$P_{\mathcal{C}_1} = [\sin(g)]^2, \tag{A3}$$

which is approximate to g^2 for $g \ll 1$. g as observed in Refs. [16,71] is of order 10^{-4}, so $P_{\mathcal{C}_1} \approx 10^{-8}$.

When the input $|\psi\rangle_{\text{in}}$ is a vacuum state, the output in modes 1 and 2 in Eq. 5 will be strictly vacuum and no photons will be detected in path 1. However, this detection event can also happen in the output in Eq. (A2) when $|\psi\rangle_{\text{in}}$ is a single photon. Therefore, there is no distinct photon detection pattern for the case of a vacuum input state; in other words, the scheme of concern cannot certify a vacuum state.

Recovery of a lossy input photon

We make use of this certification scheme to reduce the effect of transmission loss on a single photon transmitted through a lossy quantum channel as considered in Sec. III A. Given the lossy input photon in Eq. (11), we repeat the above calculations and obtain the spontaneous-PDC output

$$\delta_0|0, 0, 0\rangle_{\text{in}12}\langle 0, 0, 0| + \delta_1|\Omega\rangle_{\text{in}12}\langle\Omega|, \tag{A4}$$

where $|\Omega\rangle_{\text{in}12}$ is given in Eq. (A2). We also reiterate measurement on mode 1 in the diagonal basis, which again projects mode 2 into $\alpha|H\rangle_2 \pm \beta|V\rangle_2$. Therefore, in this lossy scenario the certification scheme of interest works the same as before but with a reduced success probability given by

$$P_{\mathcal{C}_1,\text{rec}} = \delta_1[\sin(g)]^2. \tag{A5}$$

The fidelity between the final state in mode 2 and the initial input photon $|\psi\rangle_{\text{in}}$ is 1, i.e., $F_{\mathcal{C}_1,\text{rec}} = 1$.

2. Using single-rail quantum teleportation

The schematic setup of the single-photon certification scheme using single-rail quantum teleportation [17,18] is shown in Fig. 6. To analyze its working mechanism, we first recall the process of teleporting a single-rail qubit $\alpha|1\rangle_{\text{in}} + \beta|0\rangle_{\text{in}}$ to one mode, say, mode 2, of a single-rail entangled quantum channel $c|1\rangle_1|0\rangle_2 + d|0\rangle_1|1\rangle_2$, where $|c|^2 + |d|^2 = 1$. A Bell measurement is performed on modes in and 1 by interfering their photons on a balanced beam splitter (BBS), that produces the output state

$$\begin{aligned}&\frac{\alpha c}{\sqrt{2}}(|2\rangle_3 - |2\rangle_4)|0\rangle_2 + \frac{\alpha d}{\sqrt{2}}(|1\rangle_3 + |1\rangle_4)|1\rangle_2 \\ &\quad + \frac{\beta c}{\sqrt{2}}(|1\rangle_3 - |1\rangle_4)|0\rangle_2 + \beta d|0\rangle_3|0\rangle_4|1\rangle_2.\end{aligned} \tag{A6}$$

Detection of one photon in mode 3 projects mode 2 onto an un-normalized outcome state $\alpha d|1\rangle_2 + \beta c|0\rangle_2$, while that in mode 4 projects mode 2 onto $\alpha d|1\rangle_2 - \beta c|0\rangle_2$. This can be described by a map

$$\alpha|1\rangle_{\text{in}} + \beta|0\rangle_{\text{in}} \xrightarrow{c|1\rangle_1|0\rangle_2 + d|0\rangle_1|1\rangle_2} \alpha d|1\rangle_2 \pm \beta c|0\rangle_2, \tag{A7}$$

where we have marked the subscripts of the teleported and target modes in red. One remarkable finding from this map is that assuming tunable c and d one can adjust these parameters such that $|\alpha d| \gg |\beta c|$, thus suppressing the vacuum component while amplifying the single-photon one in the final state

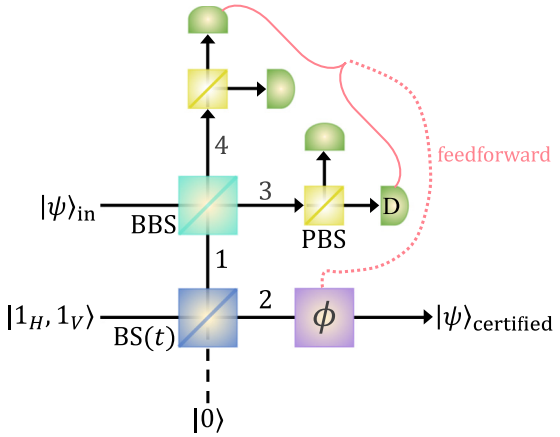

FIG. 6. Certification of a single photon using quantum teleportation of single-rail qubits. The input photon $|\psi\rangle_{\text{in}}$ in Eq. (1) is teleported to mode 2 of auxiliary single-rail entanglements created by sending two photons $|1_H, 1_V\rangle$ through a BS with transmittance t. Two single-rail Bell measurements performed on the input mode and mode 1 result in different detection patterns on photons in modes 3 and 4. Depending on these, the certified output state requires a phase feedforward correction (ϕ).

$\alpha d|1\rangle_2 \pm \beta c|0\rangle_2$. By doing this, we have performed noiseless single-photon amplification [72].

Another insight from Eq. (A7) is that tuning c and d such that $|\alpha d| \ll |\beta c|$ will suppress the single-photon component in mode 2 and therefore effectively certify a vacuum input state.

We also note that the teleportation map in Eq. (A7) remains basically unchanged when mode in is entangled with some other modes. That is, if the input state is $\alpha|1\rangle_{\text{in}}|\Theta_1\rangle + \beta|0\rangle_{\text{in}}|\Theta_0\rangle$, the (un-normalized) final state will be $\alpha d|1\rangle_2|\Theta_1\rangle \pm \beta c|0\rangle_c|\Theta_0\rangle$ corresponding to detection of one photon in mode 3 or 4. We describe this by a map:

$$\alpha|1\rangle_{\text{in}}|\Theta_1\rangle + \beta|0\rangle_{\text{in}}|\Theta_0\rangle \xrightarrow{c|1\rangle_1|0\rangle_2+d|0\rangle_1|1\rangle_2} \alpha d|1\rangle_2|\Theta_1\rangle \pm \beta c|0\rangle_2|\Theta_0\rangle. \quad \text{(A8)}$$

We are now ready to explain the certification scheme in Refs. [17,18]. We first rewrite the dual-rail input photon as $|\psi\rangle_{\text{in}} = \alpha|1_H\rangle_{\text{in}}|0_V\rangle_{\text{in}} + \beta|0_H\rangle_{\text{in}}|1_V\rangle_{\text{in}}$. We also send two auxiliary photons $|1_H, 1_V\rangle_a$ through a BS with a transmittance t to create two separate single-rail entanglements:

$$(\sqrt{1-t}|1_H\rangle_1|0_H\rangle_2 + \sqrt{t}|0_H\rangle_1|1_H\rangle_2) \otimes (\sqrt{1-t}|1_V\rangle_1|0_V\rangle_2 + \sqrt{t}|0_V\rangle_1|1_V\rangle_2). \quad \text{(A9)}$$

Using the horizontal part in Eq. (A9) as a quantum channel, we teleport the horizontal part of $|\psi\rangle_{\text{in}}$ to mode 2. Following the map in Eq. (A8), we find

$$\alpha|1_H\rangle_{\text{in}}|0_V\rangle_{\text{in}} + \beta|0_H\rangle_{\text{in}}|1_V\rangle_{\text{in}} \xrightarrow{\sqrt{1-t}|1_H\rangle_1|0_H\rangle_2+\sqrt{t}|0_H\rangle_1|1_H\rangle_2} \times \alpha\sqrt{t}|1_H\rangle_2|0_V\rangle_{\text{in}} \pm \beta\sqrt{1-t}|0_H\rangle_2|1_V\rangle_{\text{in}}. \quad \text{(A10)}$$

We next teleport the vertical part of this output state using the vertical single-rail entanglement in Eq. (A9):

$$\alpha\sqrt{t}|1_H\rangle_2|0_V\rangle_{\text{in}} \pm \beta\sqrt{1-t}|0_H\rangle_2|1_V\rangle_{\text{in}} \xrightarrow{\sqrt{1-t}|1_V\rangle_1|0_V\rangle_2+\sqrt{t}|0_V\rangle_1|1_V\rangle_2} \pm \alpha\sqrt{t(1-t)}|1_H\rangle_2|0_V\rangle_2 \pm \beta\sqrt{t(1-t)}|0_H\rangle_2|1_V\rangle_2. \quad \text{(A11)}$$

This final state is unitarily equivalent to $|\psi\rangle_{\text{in}}$.

The total success probability of this scheme is

$$P_{\mathcal{C}_2} = t(1-t) \times P_{\text{single photons}}, \quad \text{(A12)}$$

where $P_{\text{single photons}}$ represents the probability for generating the two auxiliary single photons. For a deterministic single-photon source such as a semiconductor quantum-dot emitter [73], $P_{\text{single photons}} = 1$ so $P_{\mathcal{C}_2} \approx 10^{-1}$. For a probabilistic single-photon source such as a spontaneous PDC crystal [33,34], $P_{\text{single photons}} \approx 10^{-3}$ so $P_{\mathcal{C}_2} \approx 10^{-4}$.

Recovery of a lossy input photon

We make use of this certification scheme to reduce the effect of transmission loss on a single photon transmitted through a lossy quantum channel as considered in Sec. III A. Given the lossy input photon in Eq. (11), we repeat the above calculations and obtain the final mixed state after a successful detection and a corresponding phase feedforward correction [17]:

$$\tfrac{1}{4}\delta_0(1-t)^2|0\rangle_2\langle 0| + \tfrac{1}{4}\delta_1 t(1-t)|\psi\rangle_2\langle\psi|. \quad \text{(A13)}$$

The success probability for this to happen and the fidelity between the final mixed state and initial pure state are

$$P_{\mathcal{C}_2,\text{rec}} = \delta_0(1-t)^2 + \delta_1 t(1-t), \quad \text{(A14)}$$

$$F_{\mathcal{C}_2,\text{rec}} = \frac{\delta_1 t}{\delta_0(1-t) + \delta_1 t}, \quad \text{(A15)}$$

where we assume $P_{\text{single photons}} = 1$. For $t \to 1$, we find $F_{\mathcal{C}_2,\text{rec}}$ approaches 1 but $P_{\mathcal{C}_2,\text{rec}}$ tends to zero.

3. Using dual-rail quantum teleportation

The schematic setup of the single-photon certification scheme using dual-rail quantum teleportation [19,20] is shown in Fig. 7. In particular, we perform a Bell measurement on mode in and mode 1 of the Bell pair $|\Psi^+\rangle_{12} = (|H\rangle_1|V\rangle_2 + |V\rangle_1|H\rangle_2)/\sqrt{2}$ by interfering their photons on a BBS and performing photon detection afterwards. Mathematically, we have

$$\begin{aligned}|\psi\rangle_{\text{in}}|\Psi^+\rangle_{12} \xrightarrow{\text{BBS}_{\text{in},1}} & \frac{\alpha}{\sqrt{2}}(|2_H\rangle_3|0\rangle_4 - |0\rangle_3|2_H\rangle_4)|V\rangle_2 \\ & + \frac{\alpha}{2}(|H\rangle_3 + |H\rangle_4)(|V\rangle_3 - |V\rangle_4)|H\rangle_2 \\ & + \frac{\beta}{\sqrt{2}}(|2_V\rangle_3|0\rangle_4 - |0\rangle_3|2_V\rangle_4)|V\rangle_2 \\ & + \frac{\beta}{2}(|V\rangle_3 + |V\rangle_4)(|H\rangle_3 - |H\rangle_4)|H\rangle_2. \end{aligned} \quad \text{(A16)}$$

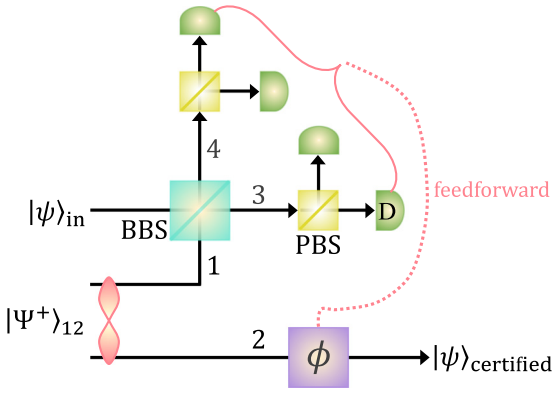

FIG. 7. Certification of a single photon using quantum teleportation of a dual-rail qubit. The input photon $|\psi\rangle_{\text{in}}$ in Eq. (1) is teleported to mode 2 of an auxiliary dual-rail Bell pair, $|\Psi^+\rangle_{12} = (|H\rangle_1|V\rangle_2 + |V\rangle_1|H\rangle_2)/\sqrt{2}$. A dual-rail Bell measurement performed on the input mode and mode 1 results in different detection patterns on photons in modes 3 and 4. Depending on these, the certified output state requires a phase feedforward correction (ϕ).

Photon detections of modes 3 and 4 in the state $|H\rangle_3|V\rangle_3$ or $|H\rangle_4|V\rangle_4$ will project mode 2 onto $\alpha|H\rangle_2 + \beta|H\rangle_2$, while those being $|H\rangle_3|V\rangle_4$ and $|V\rangle_3|H\rangle_4$ will project mode 2 onto $\alpha|H\rangle_2 - \beta|V\rangle_2$. The latter final state needs a phase-flip correction.

The total success probability of this scheme

$$P_{\mathcal{C}_3} = 1/2 \times P_{\text{Bell pair}}, \tag{A17}$$

where $P_{\text{Bell pair}}$ represents the probability of generating the auxiliary Bell pair. For an on-demand Bell-pair source such as a semiconductor quantum-dot emitter [74–76], $P_{\text{Bell pair}}$ can be close to 1 so $P_{\mathcal{C}_3} \approx 10^{-1}$. For a probabilistic Bell-pair source such as a spontaneous PDC crystal [33,34], $P_{\text{Bell pair}} \approx 10^{-3}$ so $P_{\mathcal{C}_3} \approx 10^{-4}$.

We note that mode 2 in Eq. 7 will always be in a pure or mixed single-photon state, no matter what the state $|\psi\rangle_{\text{in}}$ is, so the scheme of interest is not applicable to certification of a vacuum state.

Recovery of a lossy input photon

We make use of this certification scheme to reduce the effect of transmission loss on a single photon transmitted through a lossy quantum channel as considered in Sec. III A. Given the lossy input photon in Eq. (11), we repeat the above calculations and obtain the final mixed state after a successful detection and a corresponding feedforward correction:

$$\tfrac{1}{4}\delta_1|\psi\rangle_2\langle\psi|, \tag{A18}$$

which after normalization is exactly the same as the initial pure photon. This is because the Bell measurement outcomes have erased the possibility of mode in being in vacuum. The success probability for this to happen and the fidelity between the final mixed state and initial pure state are

$$P_{\mathcal{C}_3,\text{rec}} = 1/2 \times \delta_1, \tag{A19}$$

$$F_{\mathcal{C}_3,\text{rec}} = 1, \tag{A20}$$

where we assume $P_{\text{Bell pair}} = 1$.

APPENDIX B: INEFFICIENT PHOTODETECTORS

.We introduce the mathematical model for detection of n photons on mode a with a quantum efficiency η as a positive operator-valued measure (POVM) operator [29,54]:

$$\hat{E}^{(n)}_{\eta,a} = \sum_{k=0}^{\infty} C^k_{n+k}\eta^n(1-\eta)^k|n+k\rangle_a\langle n+k|. \tag{B1}$$

For $\eta = 1$, $\hat{E}^{(n)}_{\eta=1,a} = |n\rangle_a\langle n|$, describing an ideal projective measurement operator; for $\eta \to 0$ and $n \neq 0$, $\hat{E}^{(n)}_{\eta\to 0,a} \to 0$, implying a complete failure of gaining any measurement information. A PNR detector with an efficiency η and capability of resolving photon numbers up to a number M is represented by a POVM with $(M+2)$ elements as

$$\begin{matrix}\text{PNR detector resolving}\\ \text{up to } M \text{ photons}\end{matrix} = \begin{cases}\hat{E}^{(j)}_{\eta,a} & \text{for } j = 0, 1, \ldots, M\\ \hat{E}^{(>M)}_{\eta,a} = \mathbb{1} - \sum_{j=0}^{M}\hat{E}^{(j)}_{\eta,a}\end{cases}. \tag{B2}$$

An on-off detector with an efficiency η is a specific case of this PNR detector with $M = 0$ and thus its corresponding POVM has two elements:

$$\text{on-off detector} = \begin{cases}\hat{E}^{(\text{off})}_{\eta,a} &= \hat{E}^{(0)}_{\eta,a}\\ \hat{E}^{(\text{on})}_{\eta,a} &= \mathbb{1} - \hat{E}^{(0)}_{\eta,a}\end{cases}. \tag{B3}$$

The measurement that represents detection of $|N_H, N_V\rangle_s$ in mode s as in Fig. 1(c) using nonideal PNR or on-off detectors is respectively given by

$$\hat{\Pi}^{(\text{PNR})}_{\eta,s} = \hat{E}^{(N)}_{\eta,s,H} \otimes \hat{E}^{(N)}_{\eta,s,V}, \tag{B4}$$

$$\hat{\Pi}^{(\text{on-off})}_{\eta,s} = \hat{E}^{(\text{on})}_{\eta,s,H} \otimes \hat{E}^{(\text{on})}_{\eta,s,V}, \tag{B5}$$

where we have added the subscripts H and V to specify photon polarization. The success probability $P^{(\text{PNR})}_{\text{cer}}$ and the fidelity $F^{(\text{PNR})}_{\text{cer}}$ of our proposed certification scheme when using PNR detectors are computed by

$$P^{(\text{PNR})}_{\text{cer}} = {}_{si}\langle\phi_{N,n}|\hat{\Pi}^{(\text{PNR})}_{\eta,s}|\phi_{N,n}\rangle_{si}, \tag{B6}$$

$$F^{(\text{PNR})}_{\text{cer}} = {}_i\langle\psi_{N,n}|\hat{\rho}^{(\text{PNR})}_i|\psi_{N,n}\rangle_i, \tag{B7}$$

where $|\psi_{N,n}\rangle$ is given in Eq. (8), $|\phi_{N,n}\rangle$ is the stimulated-PDC output in Eq. (9), and

$$\hat{\rho}^{(\text{PNR})}_i = \frac{\text{Tr}_s\left[\hat{\Pi}^{(\text{PNR})}_{\eta,s}|\phi_{N,n}\rangle_{si}\langle\phi_{N,n}|\right]}{P^{(\text{PNR})}_{\text{cer}}} \tag{B8}$$

is the reduced density operator of mode i. Similar definitions hold for $P^{(\text{on-off})}_{\text{cer}}$, $F^{(\text{on-off})}_{\text{cer}}$, and $\hat{\rho}^{(\text{on-off})}_i$.

In Fig. 8 we compute $P^{(\text{PNR})}_{\text{cer}}$, $F^{(\text{PNR})}_{\text{cer}}$, $P^{(\text{on-off})}_{\text{cer}}$, and $F^{(\text{on-off})}_{\text{cer}}$ as functions of the detector efficiency η for $N = 2$ and 3. We find that $P^{(\text{on-off})}_{\text{cer}}$ is much higher than $P^{(\text{PNR})}_{\text{cer}}$, which is understandable as on-off detectors cannot distinguish between the target detection event and the other, false ones. This

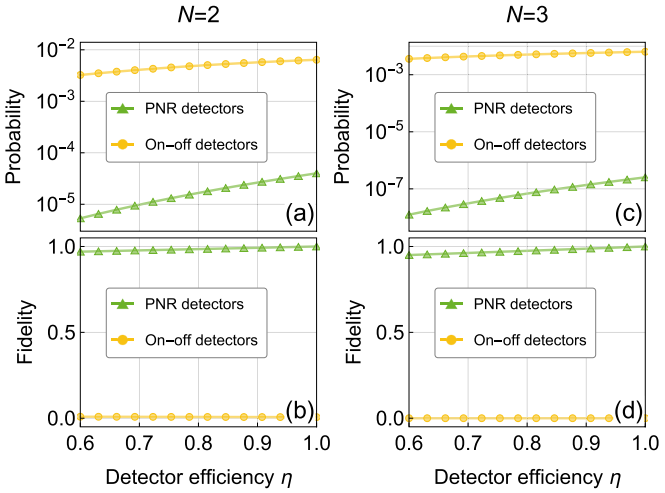

FIG. 8. (a) Success probability and (b) fidelity between the certified output state and the input state of our scheme when certifying a two-photon Fock state ($N = 2$) as functions of the detector efficiency η. We consider using both PNR (marked by filled triangles) and on-off (marked by filled circles) detectors. (c), (d) Same as (a) and (b) but for a three-photon Fock state ($N = 3$). Here the squeezing parameter $|\Gamma|$ is chosen to be 0.05.

subsequently renders $F_{\text{cer}}^{(\text{on-off})}$ irrelevant, being almost completely zero. By contrast, $F_{\text{cer}}^{(\text{PNR})}$ is very close to unit for the whole range of $\eta \in [0.6, 1]$. These highlight the essential role of PNR detectors over on-off ones in our scheme of certifying a multiphoton Fock state.

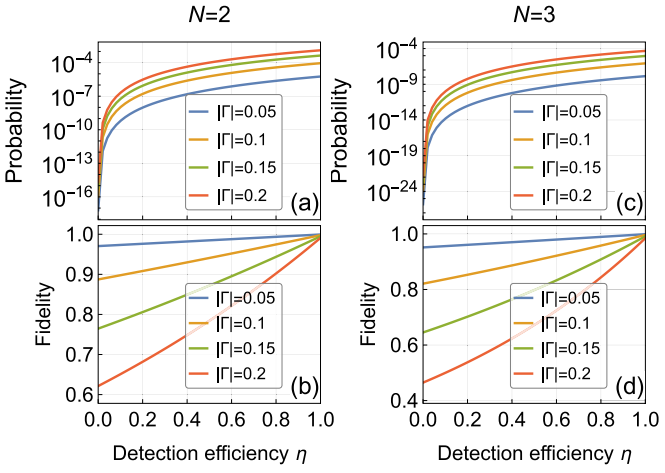

FIG. 9. (a) Success probability and (b) fidelity between the certified output state and the input state of our scheme when certifying a two-photon Fock state ($N = 2$) as functions of the detector efficiency η for different values of the squeezing parameters $|\Gamma| \in \{0.05, 0.1, 0.15, 0.2\}$. We here consider using only PNR detectors. (c, d) Same as (a) and (b) but for a three-photon Fock state ($N = 3$). We note that in the limit $\eta \to 0$ and for $|\Gamma| < 1$ the probability goes to zero, while the certification fidelity reduces to a finite nonzero value. In (a) and (b) the probabilities are arranged from bottom to top as increasing $|\Gamma|$ from 0.05 to 0.2, while in (c) and (d) the fidelities are arranged from top to bottom.

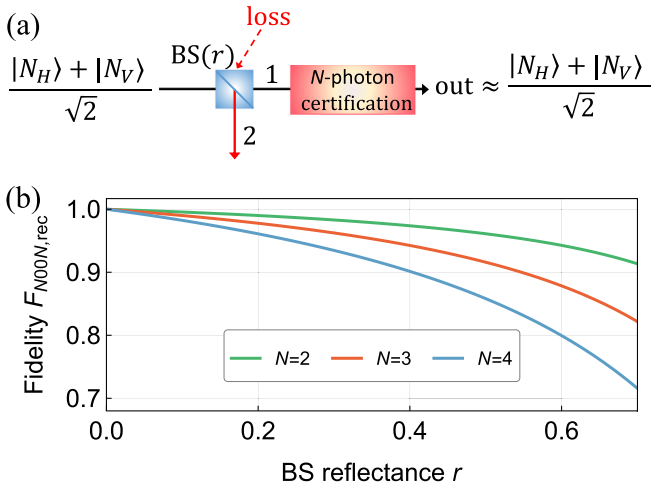

FIG. 10. (a) Due to the equivalence between path DOF and polarization DOF, the model of identical losses in both paths of a NOON state $(|N\rangle_1|0\rangle_{1'} + |0\rangle_1|N\rangle_{1'})/\sqrt{2}$ [68,69] is the same as loss in a single-mode Fock-state superposition $(|N_H\rangle_1 + |N_V\rangle_1)/\sqrt{2}$. Here loss is modeled by a BS with reflectance r. Application of our Fock-state certification scheme can recover a lossy single-mode Fock-state superposition. (b) Fidelity $F_{\text{NOON,rec}}$ given in Eq. (C8), as a function of the reflectance r for $N \in \{2, 3, 4\}$ when recovering a lossy single-mode Fock-state superposition as in (a).

In Fig. 9 we show $P_{\text{cer}}^{(\text{PNR})}$ and $F_{\text{cer}}^{(\text{PNR})}$ versus $\eta \in [0, 1]$ for different values of the squeezing parameter $|\Gamma| \in \{0.05, 0.1, 0.15, 0.2\}$. For $|\Gamma| = 0.05 \ll 1$, we observe that the certification fidelity stays close to 1 for all η. This is due to the fact that in such limit high-photon-number terms in mode s of the stimulated-PDC output are almost negligible compared to the desire detection term $|N_H, N_V\rangle_s$. False-detection probability resulting from inefficiency of PNR photodetectors is subsequently very small, making the certification fidelity very high. Therefore, realistically imperfect PNR detectors are sufficient for a high-quality multiphoton certification using our scheme. When increasing $|\Gamma|$ to 0.2, the success probability is improved but the certification fidelity becomes worse. This is because a stronger squeezing enhances the populations of higher-order multiphoton terms, which subsequently contribute more to false positives or dark counts that degrade the certification fidelity of our scheme.

APPENDIX C: RECOVERY OF A LOSSY NOON STATE

Consider a NOON state $(|N\rangle_1|0\rangle_{1'} + |0\rangle_1|N\rangle_{1'})/\sqrt{2}$ that is about to experience loss in both paths 1 and $1'$ (here we assume that losses in the two paths are identical). Because of the equivalence between path and polarization DOFs, this is the same as a polarized Fock-state superposition $(|N_H\rangle_1 + |N_V\rangle_1)/\sqrt{2}$ in mode 1 being sent through a single lossy quantum channel.

We model the effect of loss by a BS [67] with reflectance r (and transmittance $t = 1 - r$), as demonstrated in Fig. 10(a). The larger r is, the more lossy the quantum channel is. This

transforms the single-mode Fock-state superposition state to

$$\frac{1}{\sqrt{2}}(|N_H\rangle_1+|N_V\rangle_1)=\frac{1}{\sqrt{2}}\left(\frac{(\hat{a}^\dagger_{1,H})^N}{\sqrt{N!}}+\frac{(\hat{a}^\dagger_{1,V})^N}{\sqrt{N!}}\right)|0\rangle \xrightarrow{\mathrm{BS}(r)} \frac{1}{\sqrt{2}}\left[\frac{(\sqrt{t}a^\dagger_{1,H}+\sqrt{r}a^\dagger_{2,H})^N}{\sqrt{N!}}+\frac{(\sqrt{t}a^\dagger_{1,V}+\sqrt{r}a^\dagger_{2,V})^N}{\sqrt{N!}}\right]|0\rangle.$$

We express the right-hand side of the above equation explicitly in Fock-state representation:

$$\sum_{n=0}^{N} f_{n,r}[|n_H\rangle_1|(N-n)_H\rangle_2+|n_V\rangle_1|(N-n)_V\rangle_2], \tag{C1}$$

where

$$f_{n,r}=\frac{C_N^n}{\sqrt{2(N!)}}[n!(N-n)!]^{1/2}t^{n/2}r^{(N-n)/2}. \tag{C2}$$

This, after tracing out mode 2, results in mode 1 being in an un-normalized mixed state:

$$2|f_{0,r}|^2|0\rangle_1\langle 0|+\sum_{n=1}^{N-1}|f_{n,r}|^2(|n_H\rangle_1\langle n_H|+|n_V\rangle_1\langle n_V|) + |f_{N,r}|^2(|N_H\rangle+|N_V\rangle)_1(\langle N_H|+\langle N_V|). \tag{C3}$$

We then perform our N-photon Fock-state certification on mode 1. Namely, we take the mixed state in Eq. (C3) as the seed to mode s in the setup of Fig. 1(c). The corresponding stimulated-PDC output reads

$$2|f_{0,r}|^2|\ominus_{0,0}\rangle_{si}\langle\Psi_{0,0}|+\sum_{n=1}^{N-1}|f_{n,r}|^2\big(|\ominus_{n,0}\rangle_{si}\langle\Psi_{n,0}| + |\ominus_{0,n}\rangle_{si}\langle\Psi_{0,n}|\big)+|f_{N,r}|^2|\Psi_{\mathrm{NOON}}\rangle_{si}\langle\Psi_{\mathrm{NOON}}|, \tag{C4}$$

where

$$|\Psi_{m,n}\rangle_{si}=\hat{S}_{si}|m_H,n_V\rangle_s|0\rangle_i=\sum_{k,l=0}^{\infty}c^{k,l}_{m,n}|(m+k)_H,(n+l)_V\rangle_s|l_H,k_V\rangle_i, \tag{C5}$$

$$|\Psi_{\mathrm{NOON}}\rangle_{si}=\hat{S}_{si}(|N_H\rangle+|N_V\rangle)_s|0\rangle_i=\sum_{k,l=0}^{\infty}\big(c^{k,l}_{0,N}|(N+k)_H,l_V\rangle_s|l_H,k_V\rangle_i + c^{k,l}_{N,0}|k_H,(N+l)_V\rangle_s|l_H,k_V\rangle_i\big). \tag{C6}$$

Within the mixed state in Eq. (C4), we postselect mode s in the state $|N_H,N_V\rangle_s$, which collapses in mode i onto the following (un-normalized) output:

$$2\big|f_{0,r}c^{N,N}_{0,0}\big|^2|N_H,N_V\rangle_i\langle N_H,N_V| + \sum_{n=1}^{N-1}\big|f_{n,r}c^{N-n,N}_{n,0}\big|^2\big(|N_H,(N-n)_V\rangle_i\langle N_H,(N-n)_V| + |(N-n)_H,N_V\rangle_i\langle(N-n)_H,N_V|\big) + \big|f_{N,r}c^{0,N}_{N,0}\big|^2(|N_H\rangle+|N_V\rangle)_i(\langle N_H|+\langle N_V|). \tag{C7}$$

The fidelity between the mixed state in Eq. (C7) and the initial Fock-state superposition is given by

$$F_{\mathrm{NOON,rec}}=\frac{\big|f_{N,r}c^{0,N}_{N,0}\big|^2}{\big|f_{N,r}c^{0,N}_{N,0}\big|^2+\sum_{n=0}^{N-1}\big|f_{n,r}c^{N-n,N}_{n,0}\big|^2}. \tag{C8}$$

In Fig. 10(b) we plot the fidelity $F_{\mathrm{NOON,rec}}$ as a function of the reflectance r. For $r\lesssim 0.4$ we find that $F_{\mathrm{NOON,rec}}$ is close to 0.9 or higher for all $N\in\{2,3,4\}$. This demonstrates that our Fock-state certification scheme is suitable for restoring a lossy NOON state with high fidelity.

[1] J. Barrett, L. Hardy, and A. Kent, Phys. Rev. Lett. **95**, 010503 (2005).
[2] U. Vazirani and T. Vidick, Phys. Rev. Lett. **113**, 140501 (2014).
[3] S. Pironio, A. Acín, S. Massar, A. B. de la Giroday, D. N. Matsukevich, P. Maunz, S. Olmschenk, D. Hayes, L. Luo, T. A. Manning, and C. Monroe, Nature (London) **464**, 1021 (2010).
[4] A. Acín and L. Masanes, Nature (London) **540**, 213 (2016).
[5] S. J. Freedman and J. F. Clauser, Phys. Rev. Lett. **28**, 938 (1972).
[6] G. Weihs, T. Jennewein, C. Simon, H. Weinfurter, and A. Zeilinger, Phys. Rev. Lett. **81**, 5039 (1998).
[7] M. Scully and M. Zubairy, *Quantum Optics*, Quantum Optics (Cambridge University, Cambridge, England, 1997).
[8] P. Grangier, J. A. Levenson, and J.-P. Poizat, Nature (London) **396**, 537 (1998).
[9] N. Imoto, H. A. Haus, and Y. Yamamoto, Phys. Rev. A **32**, 2287 (1985).
[10] J. H. Shapiro, Phys. Rev. A **73**, 062305 (2006).
[11] J. Gea-Banacloche, Phys. Rev. A **81**, 043823 (2010).
[12] A. Reiserer, S. Ritter, and G. Rempe, Science **342**, 1349 (2013).
[13] D. Niemietz, P. Farrera, S. Langenfeld, and G. Rempe, Nature (London) **591**, 570 (2021).
[14] E. Distante, S. Daiss, S. Langenfeld, L. Hartung, P. Thomas, O. Morin, G. Rempe, and S. Welte, Phys. Rev. Lett. **126**, 253603 (2021).
[15] A. Cabello and F. Sciarrino, Phys. Rev. X **2**, 021010 (2012).
[16] E. Meyer-Scott, D. McCloskey, K. Gołos, J. Z. Salvail, K. A. G. Fisher, D. R. Hamel, A. Cabello, K. J. Resch, and T. Jennewein, Phys. Rev. Lett. **116**, 070501 (2016).
[17] N. Gisin, S. Pironio, and N. Sangouard, Phys. Rev. Lett. **105**, 070501 (2010).
[18] S. Kocsis, G. Y. Xiang, T. C. Ralph, and G. J. Pryde, Nat. Phys. **9**, 23 (2013).
[19] P. Kok, H. Lee, and J. P. Dowling, Phys. Rev. A **66**, 063814 (2002).
[20] X.-L. Wang, X.-D. Cai, Z.-E. Su, M.-C. Chen, D. Wu, L. Li, N.-L. Liu, C.-Y. Lu, and J.-W. Pan, Nature (London) **518**, 516 (2015).

[21] C. Gerry and P. Knight, *Introductory Quantum Optics* (Cambridge University, Cambridge, England, 2004).
[22] S. A. Podoshvedov, J. Noh, and K. Kim, Opt. Commun. **232**, 357 (2004).
[23] A. Lamas-Linares, C. Simon, J. C. Howell, and D. Bouwmeester, Science **296**, 712 (2002).
[24] K. J. Resch, J. S. Lundeen, and A. M. Steinberg, Phys. Rev. Lett. **88**, 113601 (2002).
[25] A. Zavatta, S. Viciani, and M. Bellini, Science **306**, 660 (2004).
[26] V. Parigi, A. Zavatta, M. Kim, and M. Bellini, Science **317**, 1890 (2007).
[27] J. J. Guanzon, M. S. Winnel, A. P. Lund, and T. C. Ralph, Phys. Rev. Lett. **128**, 160501 (2022).
[28] P. G. Kwiat, K. Mattle, H. Weinfurter, A. Zeilinger, A. V. Sergienko, and Y. Shih, Phys. Rev. Lett. **75**, 4337 (1995).
[29] P. Kok and B. W. Lovett, *Introduction to Optical Quantum Information Processing* (Cambridge University, Cambridge, England, 2010).
[30] C. Couteau, Contemp. Phys. **59**, 291 (2018).
[31] D. T. Le, W. Asavanant, and N. B. An, Phys. Rev. A **104**, 012612 (2021).
[32] C. Simon, G. Weihs, and A. Zeilinger, Phys. Rev. Lett. **84**, 2993 (2000).
[33] S. Fasel, O. Alibart, S. Tanzilli, P. Baldi, A. Beveratos, N. Gisin, and H. Zbinden, New J. Phys. **6**, 163 (2004).
[34] P. G. Kwiat and R. Y. Chiao, Phys. Rev. Lett. **66**, 588 (1991).
[35] C. M. Nunn, J. D. Franson, and T. B. Pittman, Phys. Rev. A **104**, 033717 (2021).
[36] H. F. Hofmann, Phys. Rev. A **79**, 033822 (2009).
[37] A. E. Lita, A. J. Miller, and S. W. Nam, Opt. Express **16**, 3032 (2008).
[38] G. S. Thekkadath, M. E. Mycroft, B. A. Bell, C. G. Wade, A. Eckstein, D. S. Phillips, R. B. Patel, A. Buraczewski, A. E. Lita, T. Gerrits, S. W. Nam, M. Stobińska, A. I. Lvovsky, and I. A. Walmsley, npj Quantum Inf. **6**, 89 (2020).
[39] J. M. Arrazola, V. Bergholm, K. Brádler, T. R. Bromley, M. J. Collins, I. Dhand, A. Fumagalli, T. Gerrits, A. Goussev, L. G. Helt, J. Hundal, T. Isacsson, R. B. Israel, J. Izaac, S. Jahangiri, R. Janik, N. Killoran, S. P. Kumar, J. Lavoie, A. E. Lita *et al.*, Nature (London) **591**, 54 (2021).
[40] Y. Israel, L. Cohen, X.-B. Song, J. Joo, H. S. Eisenberg, and Y. Silberberg, Optica **6**, 753 (2019).
[41] M. Jönsson and G. Björk, Phys. Rev. A **99**, 043822 (2019).
[42] J. Provazník, L. Lachman, R. Filip, and P. Marek, Opt. Express **28**, 14839 (2020).
[43] R. Nehra, C.-H. Chang, Q. Yu, A. Beling, and O. Pfister, Opt. Express **28**, 3660 (2020).
[44] M. Endo, T. Sonoyama, M. Matsuyama, F. Okamoto, S. Miki, M. Yabuno, F. China, H. Terai, and A. Furusawa, Opt. Express **29**, 11728 (2021).
[45] S. Barz, G. Cronenberg, A. Zeilinger, and P. Walther, Nat. Photonics **4**, 553 (2010).
[46] C. Wagenknecht, C.-M. Li, A. Reingruber, X.-H. Bao, A. Goebel, Y.-A. Chen, Q. Zhang, K. Chen, and J.-W. Pan, Nat. Photonics **4**, 549 (2010).
[47] M. J. Holland and K. Burnett, Phys. Rev. Lett. **71**, 1355 (1993).
[48] K. Banaszek and P. L. Knight, Phys. Rev. A **55**, 2368 (1997).
[49] J.-W. Pan, D. Bouwmeester, M. Daniell, H. Weinfurter, and A. Zeilinger, Nature (London) **403**, 515 (2000).
[50] E. Bimbard, N. Jain, A. MacRae, and A. I. Lvovsky, Nat. Photonics **4**, 243 (2010).
[51] M. Cooper, L. J. Wright, C. Söller, and B. J. Smith, Opt. Express **21**, 5309 (2013).
[52] D. T. Pegg, L. S. Phillips, and S. M. Barnett, Phys. Rev. Lett. **81**, 1604 (1998).
[53] M. S. Winnel, N. Hosseinidehaj, and T. C. Ralph, Phys. Rev. A **102**, 063715 (2020).
[54] D. T. Le, C. T. Bich, and N. B. An, Optik **225**, 165820 (2021).
[55] B. Schumacher and M. A. Nielsen, Phys. Rev. A **54**, 2629 (1996).
[56] R. García-Patrón, S. Pirandola, S. Lloyd, and J. H. Shapiro, Phys. Rev. Lett. **102**, 210501 (2009).
[57] M. S. Winnel, J. J. Guanzon, N. Hosseinidehaj, and T. C. Ralph, npj Quantum Inf. **8**, 129 (2022).
[58] M. Kacprowicz, R. Demkowicz-Dobrzański, W. Wasilewski, K. Banaszek, and I. A. Walmsley, Nat. Photonics **4**, 357 (2010).
[59] K. Jiang, C. J. Brignac, Y. Weng, M. B. Kim, H. Lee, and J. P. Dowling, Phys. Rev. A **86**, 013826 (2012).
[60] B. Liu and Z. Y. Ou, Phys. Rev. A **74**, 035802 (2006).
[61] F. W. Sun, Z. Y. Ou, and G. C. Guo, Phys. Rev. A **73**, 023808 (2006).
[62] H. F. Hofmann and T. Ono, Phys. Rev. A **76**, 031806(R) (2007).
[63] G. J. Pryde and A. G. White, Phys. Rev. A **68**, 052315 (2003).
[64] H. Cable and J. P. Dowling, Phys. Rev. Lett. **99**, 163604 (2007).
[65] J. C. F. Matthews, A. Politi, D. Bonneau, and J. L. O'Brien, Phys. Rev. Lett. **107**, 163602 (2011).
[66] Y.-S. Ra, H.-T. Lim, J.-E. Oh, and Y.-H. Kim, Opt. Express **23**, 30807 (2015).
[67] S. D. Huver, C. F. Wildfeuer, and J. P. Dowling, Phys. Rev. A **78**, 063828 (2008).
[68] T.-W. Lee, S. D. Huver, H. Lee, L. Kaplan, S. B. McCracken, C. Min, D. B. Uskov, C. F. Wildfeuer, G. Veronis, and J. P. Dowling, Phys. Rev. A **80**, 063803 (2009).
[69] B. Roy Bardhan, K. Jiang, and J. P. Dowling, Phys. Rev. A **88**, 023857 (2013).
[70] M. Curty and T. Moroder, Phys. Rev. A **84**, 010304(R) (2011).
[71] N. K. Langford, T. J. Weinhold, R. Prevedel, A. Gilchrist, J. L. O'Brien, G. J. Pryde, and A. G. White, Phys. Rev. Lett. **95**, 210504 (2005).
[72] T. C. Ralph and A. P. Lund, AIP Conf. Proc. **1110**, 155 (2009).
[73] P. Senellart, G. Solomon, and A. White, Nat. Nanotechnol. **12**, 1026 (2017).
[74] M. Müller, S. Bounouar, K. D. Jöns, M. Glässl, and P. Michler, Nat. Photonics **8**, 224 (2014).
[75] D. Huber, M. Reindl, S. F. Covre da Silva, C. Schimpf, J. Martín-Sánchez, H. Huang, G. Piredda, J. Edlinger, A. Rastelli, and R. Trotta, Phys. Rev. Lett. **121**, 033902 (2018).
[76] K. D. Zeuner, K. D. Jöns, L. Schweickert, C. Reuterskiöld Hedlund, C. Nuñez Lobato, T. Lettner, K. Wang, S. Gyger, E. Schöll, S. Steinhauer, M. Hammar, and V. Zwiller, ACS Photonics **8**, 2337 (2021).